Structures, Stabilities, and Electronic Properties of Gold Silicide Clusters: Comparison with Pure Silicon Clusters

Zhi-Jian Zhou[a] and Yan-Fei Hu[a,b]

[a] School of Science, Sichuan University of Science & Engineering, Zigong 643000, China
[b] Institute of Atomic and Molecular Physics, Sichuan University, Chengdu 610065, China

Reprint requests to Z.-J. Z.; E-mail: zhjzhouzhijian@163.com

Z. Naturforsch. **67a,** 99 – 110 (2012) / DOI: 10.5560/ZNA.2011-0061
Received April 13, 2011 / revised August 15, 2011

The local meta-GGA (generalized gradient approximation) exchange correlation density functional (TPSS) with relativistic effective core potential was employed to systematically investigate the geometric structures, stabilities, and electronic properties of bimetallic Au_2Si_n ($n = 1-8$) clusters. The optimized geometries show that the most stable isomers have a three-dimensional structure except for $Au_2Si_{1,3}$ clusters. The doped gold atoms prefer to occupy the surface site in the Au_2Si_n clusters. Here, the averaged atomic binding energies and fragmentation energies show that the Au_2Si_5 isomer is the most stable among the Au_2Si_n ($n = 1-8$) clusters. A pronounced even-odd alternation is found in the energy difference between the highest occupied and the lowest unoccupied molecular orbital (HOMO–LUMO gaps), especially, the Au_2Si_5 cluster has the largest HOMO–LUMO gap of 2.06 eV. Moreover, the reverse even–odd alternation rule to the average polarizability per atom versus the charges transfer was found. A transition point appears at $n = 5$.

Key words: Au-Si Cluster; Geometric Configuration; Density Functional Theory.

1. Introduction

Since silicon is a key semiconducting material of great importance in microelectronic industry, the silicon clusters have been extensively investigated both experimentally and theoretically [1 – 12]. However, all these results show that pure silicon clusters are unsuitable as building block because Si_n clusters tend to bind themselves against fullerene-like cages due to the sp^3 hybridization [13]. This motivates the search for a good way to achieve the production of stable silicon cage-like clusters and to introduce a metal atom, in particular a transition metal (TM) atom, in the Si_n clusters, which then dramatically change their status. Therefore, several projects of these metal-silicon clusters have been performed and investigated by many groups.

On the experimental side, the production of metal-silicon clusters $TM:Si_n$ (TM = W, Mo, and Cr) were first reported by Beck [14], who found these clusters exhibiting increased stability toward photofragmentation compared to similar sized pure silicon clusters. Recently, Hiura et al. [15] have reported experimental investigations of small mixed transition metal-silicon $TM:Si_n$ (TM = Hf, Ta, W, Re, Ir; n = 14, 13, 12, 11, 9) clusters. Scherer et al. [16 – 18] have produced mixed coinage metal-silicon clusters by time-of-flight mass spectroscopy and studied the electronic states of CuSi, AgSi, and AuSi dimers by measuring their laser absorption spectra. In addition, the anionic V_2Si_n and Sc_2Si_n ($n = 2-6$) clusters have been investigated by photoelectron spectroscopy (PES) and density functional theory (DFT) [19, 20].

Theoretically, Lu and Nagase [21] computed $TM:Si_n$ (TM = W, Zr, Os, Pt, Co, etc.) and revealed that the formation of an endohedral structure strongly depends on the size of the Si_n clusters. Turski [22] and Turski and Barysz [23] investigated M : Si (M = Cu, Ag, Au) by using the complete active space self-consistent field (CASSCF) method [22, 23]. Many properties of metal-doped silicon clusters, including growth behaviour, stability, magnetism, and structure, have been systematically investigated by Kumar and co-workers [24 – 27] and Zdetsis [28, 29]. Han and co-workers [30 – 36] performed calculations on $M:Si_n$ (M = Cr, W, Ir, Ag; $n = 1-6$) and $M:Si_n$ (M = Re,

Ta, Zr; $n = 1-12$) clusters. Kiran et al. [37] reported a systematic research on $SiAu_n$ ($n = 2-4$) clusters and found that a single gold atom behaves like hydrogen in its bonding to silicon. Very recently, Wang et al. [38] have studied the structures and stabilities of $AuSi_n$ ($n = 1-16$) clusters. For silicon clusters doped with double transition metal atoms, some theoretical studies are carried out. For instance, the structure and magnetic properties of neutral and anionic T_2Si_n (T = Fe, Co, Ni, Cr, and Mn; $1 \leq n \leq 8$) clusters have been investigated by Robles and Khanna [39, 40]. Li et al. [41] reported the structure and bonding of neutral and anionic Si_2Au_n ($n = 2$ and 4) clusters. The stabilities and charge-transfer of Mo_2Si_n ($n = 9-16$) cluster are also investigated by Han et al. [42]. However, to the best of our knowledge, few systematic investigations of Au_2Si_n ($n = 1-8$) clusters have been performed. For example, if two gold atoms are doped in the silicon clusters, do their structures and properties differ from those of the bare silicon clusters? Hence it is of interest to report a density functional theory investigation to reveal the geometries, stability, and electronic properties of the small size bimetallic Au_2Si_n ($n = 1-8$) clusters. We find some interesting tendencies in the geometric structures. Furthermore, the averaged atomic binding energies and fragmentation energies show that the Au_2Si_5 isomer is the most stable structure for Au_2Si_n ($n = 1-8$) clusters. In addition, the HOMO–LUMO gap, charge transfer, and polarizability were also analyzed and further compared.

2. Theoretical Methods and Computational Details

All optimizations were performed using the GAUSSIAN 03 program package [43] at TPSS level [44]. Because the TPSS functional include the kinetic energy density in the functional expression, more accurate results both for the atomization energy and for the relative stability of competing isomers are produced. The basis sets (termed GENECP) were then combinations of the 6-311+G (d) [45] and LANL2TZ (f) [46] basis sets employed for the silicon and gold atoms, respectively. In searching for the lowest-energy structures of Au_2Si_n ($n = 1-8$) clusters, lots of possible initial structures were considered, starting from the previous optimized Si_n, $TM:Si_n$, and M_2Si_n geometries [6–12, 21–23, 29–34, 42], and all clusters were relaxed fully without any symmetry constraints. In this way, a large number of optimized isomers for Au_2Si_n ($n = 1-8$) clusters were obtained. Here, we only report on a few low-lying isomers, but many higher energy structures are shown in the appendix.

To test the reliability of our calculations, we first carried out a comparison by employing different density functions and basis sets for the small clusters AuSi, Au_2, and Si_2. The results are listed in Table 1. From the table, one can see that the results based on the TPSS function and 6-311+G (d), LANL2TZ (f) bases sets are in good agreement with experimental results [17, 18, 47]. This indicates that the current com-

Table 1. Theoretical and experimental values of the bond lengths (r), dissociation energies (D_e), and vibration frequencies (ω_e) for the AuSi, Au_2, and Si_2 molecules.

Methods	Basis set	AuSi			Au_2			Si_2		
		r (Å)	D_e (eV)	ω_e (cm^{-1})	r (Å)	D_e (eV)	ω_e (cm^{-1})	r (Å)	D_e (eV)	ω_e (cm^{-1})
B3LYP	SDD	2.30	2.73	347.4	2.58	1.86	163.0	2.28	3.06	485.5
	Dz	2.31	2.81	346.8	2.57	1.87	162.2			
	Tz	2.29	2.88	359.6	2.56	1.93	167.6			
	Tz (f)	2.28	5.53	359.0	2.55	1.98	169.5			
B3PW91	SDD	2.28	2.77	359.7	2.55	1.89	169.6	2.27	3.13	497.1
	Dz	2.29	2.86	358.8	2.55	1.90	170.7			
	Tz	2.27	2.92	371.7	2.53	1.96	176.0			
	Tz (f)	2.27	3.13	497.1	2.52	2.02	177.9			
TPSS	SDD	2.28	3.03	365.7	2.55	2.15	171.3	**2.17**	**3.17**	**539.3**
	Dz	2.29	3.14	364.6	2.54	2.19	174.3			
	Tz	2.27	3.20	376.9	2.53	2.25	178.9			
	Tz (f)	**2.26**	**3.22**	**376.0**	**2.51**	**2.30**	**180.7**			
Experiment		**2.26**[a]	**3.3**[a]	**400**[a]	**2.47**[b]	**2.30**[b]	**191**[b]	**2.25**[b]	**3.22**[b]	**511.0**[b]

[a] [17, 18] [b] [41]

putational method is very suitable to describe small Au-Si mixed clusters.

3. Results and Discussions

3.1. Bare Silicon Clusters Si_n $(n = 3-10)$

In order to compare the effects of the dopant atoms on the silicon clusters, we first performed some optimizations and discussions of Si_n $(n = 3-10)$ clusters. Here, the ground state silicon clusters for each size are shown in Figure 1. From the figure, one can see that the structures and electronic states are in good agreement with the previous results [6–12]. For Si_2 and Si_3 clusters, our calculated binding energies are 3.17 eV and 7.27 eV, which are in agreement with experimental values (3.22 eV and 7.4 ± 0.5 eV) [41, 48]. In addition,

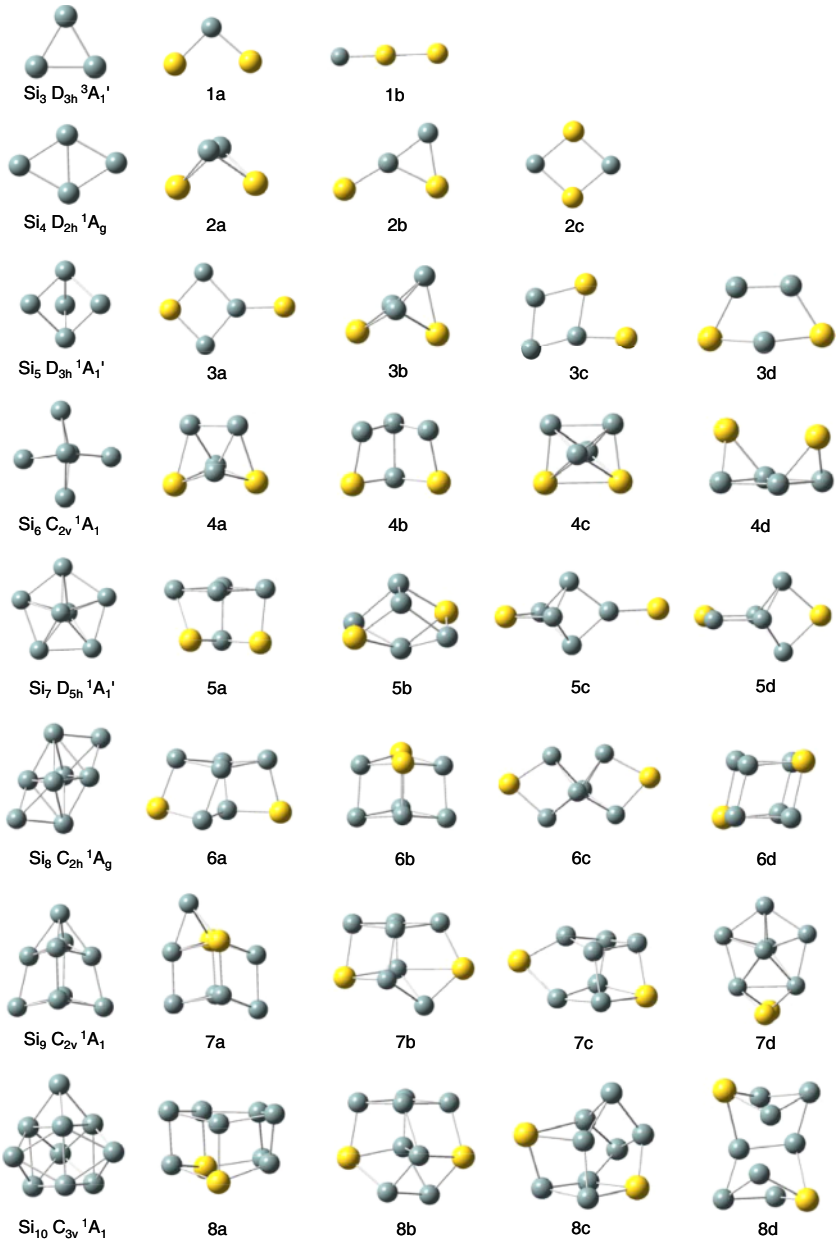

Fig. 1 (colour online). Lowest energy structure of Si_{n+2} and Au_2Si_n $(n = 1-8)$ clusters and few low-lying isomers for doped clusters. The yellow and grey balls represent gold and silicon atoms, respectively.

we find that an edge-capped trigonal bipyramid of C_{2v} symmetry is the ground state of Si_6 clusters. It accords with the results based on Hartree–Fock (HF) gradients but differs with the results of experiment and MP2 calculation [49, 50].

3.2. Bimetallic Gold-Silicon Clusters Au_2Si_n ($n = 1-8$)

For Au_2Si_n ($n = 1-8$) clusters, the ground state isomer and few low-lying structures for each size are displayed in Figure 1. Meanwhile, Table 2 lists the electronic states, symmetries, relative energies, HOMO and LUMO energies, as well as vibration frequencies of Au_2Si_n ($n = 1-8$) clusters.

All possible initial structures of Au_2Si clusters such as linear structures and triangular structures are optimized as stable structures with different spin multiplicities. According to the calculated results, the lowest-energy isomer is an obtuse-angle triangular structure (1a) with an angle of 93.6° and a $Si-Au$ bond length of 2.86 Å. For Au_2Si_2 clusters, the most stable isomer, 2a, is a dibridged structure with C_{2v} symmetry. Unlike single doped case [38], the square structure (2c) is not the lowest energy structure of Au_2Si_2 clusters because it is 0.8 eV higher in energy than 2a. Interestingly, the lowest-energy structure of Au_2Si_3 clusters is a planar structure, which has a scoop-shaped structure and C_{2v} symmetry. When the 2a isomer is capped with one silicon atom, the lowest-energy 3D isomer (3b) is obtained. Unfortunately, this structure is 0.08 eV higher in total energy than the most stable isomer 3a and its HOMO–LUMO gap (1.37 eV) is lower than that of the 3a isomer (1.93 eV). When two silicon atoms of the ground state Si_6 cluster are substituted by gold atoms, the lowest-energy isomer of Au_2Si_4 clusters (4a) with boat-like structure is generated. However, its C_{2v} symmetry is lowered to be the C_s symmetry due to the Jahn–Teller effect. Guided by the T_2Si_5 (T = Cr and Mn) clusters [40], the pentagonal bipyramid structure with C_{2v} symmetry is optimized. Whereas a frequency calculation reveals that it is a transition state with one imaginary frequency. Performing further calculation, the most stable Au_2Si_5 isomer (5a) with C_1 symmetry is obtained. This finding is similar to the Fe_2Si_5 cluster [39]. Interestingly, 5c, 5e, and 5f are three structures derived from the Si_5 cluster (D_{3h}), where two dopant gold atoms can cap the trigonal bipyramid structure in different directions. Therefore, these three isomers have different relative energies (0.60 eV, 0.95 eV, and 1.00 eV), electronic states ($^1A_1$, $^1A'$, and ^1A), and HOMO–LUMO gaps (2.15 eV, 1.59 eV, and 1.51 eV). As shown in Figure 1, the lowest-energy isomer of the Au_2Si_6 cluster (6a) can be viewed as one silicon atom added to the bottom of the 5a structure. Although two high symmetry isomers (6c and 6d) are obtained, the results of the total energy reveal that they are less stable than 6a by 0.19 and 0.50 eV, respectively. Similar to the Au_2Si_4 clusters, the most stable isomer of Au_2Si_7 clusters (7a) is a substituted structure of the Si_9 isomer; its C_{2v} symmetry drops to C_s from symmetry due to the effects of the dopant gold atoms. When one silicon atom is added to the bottom of isomer 6a, 7b is generated. But it is 0.19 eV in energy higher than the 7a structure. For Au_2Si_8 clusters, the lowest-energy isomer is a distorted pentagonal prism structure. The 8b isomer can be viewed as a silicon atom added to the bottom of isomer 7b. It is interesting that the 8c structure (C_2) is considered as two distorted boat-like structures of $AuSi_4$ isomers, and 8f (C_2) is considered as two distorted doubly-triangular pyramids of $AuSi_4$ clusters. This structure is similar to the ground state $AuSi_5$ clusters [38].

From the above discussion, it is shown that the lowest-energy configurations of $Au_2Si_{2,4-8}$ clusters have a three-dimensional (3D) structure. These structures of Au_2Si_{4-8} are similar to the corresponding ground state $AuSi_{5-9}$ clusters [38]. However, the Au_2Si_3 cluster shows planar configuration, which is different from the corresponding $AuSi_4$ cluster. The reason may be that the double doped structure is easier to keep higher symmetry than that of single doped case. In addition, we also found that the doped gold atoms prefer to occupy the surface site of Au_2Si_n clusters, which is consistent with the fact of single gold doped silicon clusters.

3.3. Relative Stabilities

In order to predict and compare relative stabilities of the most stable Si_{n+2} and Au_2Si_n ($n = 1-8$) clusters, it is worth investigating the averaged atomic binding energy $E_b(n)$ and the fragmentation energy $\Delta E(n)$, which are defined using the following formulas:

$$E_b(\mathrm{Si}_n) = \frac{nE(\mathrm{Si}) - E(\mathrm{Si}_n)}{n}, \tag{1}$$

Table 2. Electronic states, symmetries, relative energies (ΔE), HOMO energies, LUMO energies, and vibration frequencies of Au_2Si_n ($n = 1-8$) clusters.

Isomer	State	Symm.	ΔE (eV)	HOMO (hartree)	LUMO (hartree)	Frequency (cm^{-1})
1a	$^1A_1$	C_{2v}	0.00	−0.217	−0.146	47.2, 359.0, 362.5
1b	$^1\Sigma$	$C_{\infty v}$	1.55	−0.194	−0.169	33.2,168.6,425.2
2a	$^1A_1$	C_{2v}	0.00	−0.169	−0.118	51.5, 169.4, 228.3, 245.9, 441.7
2b	$^1A'$	C_s	0.47	−0.176	−0.131	45.7, 47.2, 183.7, 258.6, 293.7
2c	^3A_u	D_{2h}	0.80	−0.178	−0.150	72, 85.7, 221.7 ,259.1, 268.5
3a	$^1A_1$	D_{2h}	0.00	−0.200	−0.128	56, 75.5, 81.2, 122.1, 250.3
3b	$^1A'$	C_s	0.08	−0.189	−0.138	44.4, 12.4, 116, 171.9, 197.3
3c	$^1A'$	C_s	0.15	−0.200	−0.137	30.8, 53, 113.4, 118.5, 211.8
3d	$^1A'$	C_s	0.22	−0.193	−0.137	17.2, 96.5, 124.7, 156.9, 177
4a	^1A	C_2	0.00	−0.202	−0.152	50.4, 84.7, 102.8, 158.8, 169.2
4b	$^1A'$	C_s	0.20	−0.203	−0.164	43, 80.5, 83.4, 104.7, 144.8
4c	$^1A'$	C_{2v}	0.25	−0.202	−0.157	23.4, 59.1, 108.2, 109.4, 169.9
4d	^1A	C_2	0.28	−0.195	−0.137	22.7, 62.7, 105.5, 180.4, 198.2
5a	^1A	C_1	0.00	−0.200	−0.124	34.2, 39.7, 84.9, 112.1, 160.4
5b	^1A	C_2	0.18	−0.202	−0.132	64.1, 74.1, 83.8, 129.3, 186.9
5c	$^1A_1$	C_{2v}	0.60	−0.211	−0.133	15.9, 54.6, 73.9, 90.1, 158.6
5d	$^1A'$	C_s	0.92	−0.197	−0.149	21.6, 47.4, 60.2, 61.3, 106.1
6a	^1A	C_1	0.00	−0.199	−0.139	46.8, 54.6, 76.2, 97.3, 120.7
6b	$^1A'$	C_s	0.10	−0.197	−0.147	50.6, 59.7, 78.3, 104.9, 128.3
6c	$^1A_1$	C_{2v}	0.19	−0.190	−0.129	53.6, 54.8, 58.1, 80.3, 83.8
6d	^1A_g	C_{2h}	0.50	−0.189	−0.144	36.8, 58.1, 64, 80.8, 88.6
7a	$^1A'$	C_s	0.00	−0.192	−0.146	52.3, 66.2, 80.4, 92.3, 120.4
7b	^1A	C_1	0.19	−0.182	−0.151	50.1, 64.6, 80.7, 88.1, 117.4
7c	^1A	C_1	0.51	−0.184	−0.144	29.7, 62, 84.9, 91.1, 100.7
7d	$^1A_1$	C_{2v}	0.61	−0.183	−0.141	18.2, 54.6, 63.9, 76, 103.6
8a	^1A	C_1	0.00	−0.197	−0.140	46.2, 65.6, 85.5, 89.6, 113
8b	^1A	C_1	0.51	−0.195	−0.138	43.9, 63.2, 68.6, 79.2, 99
8c	^1A	C_1	0.67	−0.193	−0.137	23.4, 46.8, 65.3, 73.8, 92
8d	^1A	C_2	0.71	−0.192	−0.130	35.3, 41.5, 52.7, 88, 93.9

$$\Delta E(\mathrm{Si}_n) = E(\mathrm{Si}_{n-1}) + E(\mathrm{Si}) - E(\mathrm{Si}_n), \quad (2)$$

$$E_b(n) = \frac{2E(\mathrm{Au}) + nE(\mathrm{Si}) - E(\mathrm{Au_2Si}_n)}{n+2}, \quad (3)$$

$$\Delta E(n) = E(\mathrm{Au_2Si}_{n-1}) + E(\mathrm{Si}) - E(\mathrm{Au_2Si}_n), \quad (4)$$

where $E(\mathrm{Si}_{n-1})$, $E(\mathrm{Au_2Si}_{n-1})$, $E(\mathrm{Si})$, $E(\mathrm{Au})$, $E(\mathrm{Si}_n)$, and $E(\mathrm{Au_2Si}_n)$ denote the total energy of the Si_{n-1}, $\mathrm{Au_2Si}_{n-1}$, Si, Au, Si_n, and $\mathrm{Au_2Si}_n$ clusters, respectively. The calculated $E_b(n)$ and $\Delta E(n)$ values are plotted against the cluster size in Figure 2. As seen in the figure, the curves of $E_b(n)$ for Si_{n+2} and $\mathrm{Au_2Si}_n$ clusters show a smooth growing trend with cluster size. Two obvious peaks are found for Si_{n+2} and $\mathrm{Au_2Si}_n$ clusters, respectively, at $n = 5$. This indicates that the clusters of Si_7 and Au_2Si_5 are more stable. Moreover, the $E_b(n)$ values of the $\mathrm{Au_2Si}_n$clusters are smaller than those of the Si_{n+2} clusters, which suggests that the double gold atoms can not enhance the stability of silicon clusters with small size. It is similar to the case of Ag-doped and Au-doped silicon clusters [33, 38]. For $\Delta E(\mathrm{Si}_n)$, we calculate the values; those are: 3.17 eV, 4.11 eV, 4.42 eV, 3.98 eV, 4.35 eV, 4.29 eV, 2.84 eV, 4.29 eV, and 4.40 eV at $n = 2-10$, respectively. It is worth noting that the calculated values for $\mathrm{Si}_{2,3,4}$ clusters agree well with experimental data (3.21 eV, 4.09 eV, and 4.60 ± 0.15 eV) [11, 47, 51]. Unfortunately, there are no experimental values for the Si_n clusters at

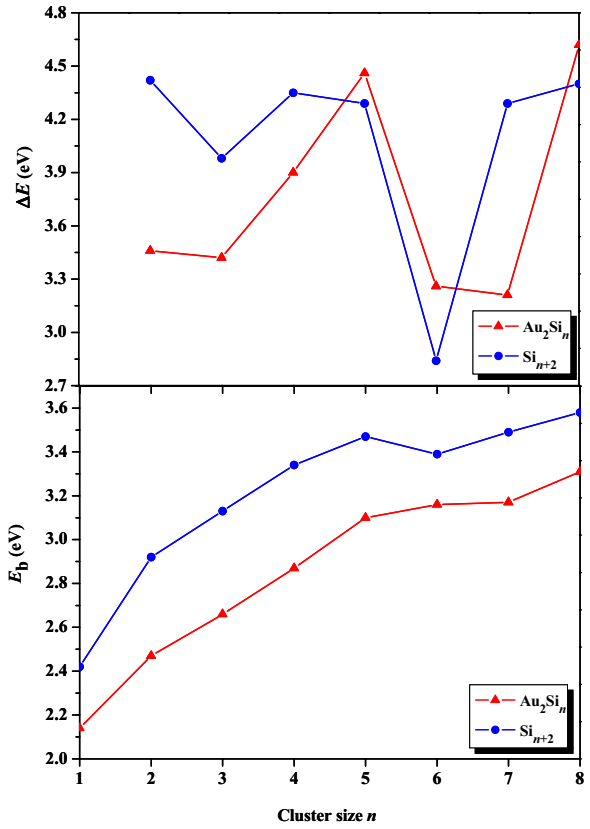

Fig. 2 (colour online). Size dependence of the averaged atomic binding energies and the fragmentation energies for the lowest energy structures of Si_{n+2} and Au_2Si_n ($n = 1-8$) clusters.

$n > 4$. Thus, we hope that our results might be useful for further experimental research. Besides, the curve of $\Delta E(n)$ for Au_2Si_n clusters display an obvious peak at $n = 5$, which is in accord with the above analysis based on the averaged atomic binding energy.

In order to confirm the stability of the Au_2Si_n clusters, we also calculated the energy differences $E_{dis}(n)$ of Au_2, Si_n, and Au_2Si_n, clusters, defined as

$$E_{dis}(n) = E(Au_2) + E(Si_n) - E(Au_2Si_n). \quad (5)$$

Here, $E(Au_2)$, $E(Si_n)$, and $E(Au_2Si_n)$ denote the total energy of the ground state Au_2, Si_n, and Au_2Si_n clusters, respectively. The energy difference curves as a function of size n for various clusters are presented in Figure 3. Similar to ΔE of Au_2Si_n clusters, $E_{dis}(n)$ displays three remarkable peaks at $n = 2$, 5, and 8, which implies that the $Au_2Si_{2,5,8}$ clusters have higher adsorption energies than the other clusters.

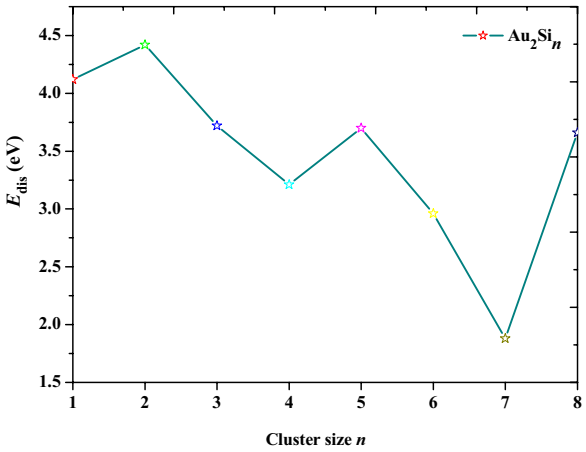

Fig. 3 (colour online). Size dependence of the energy difference for the lowest energy structure of Au_2Si_n ($n = 1-8$) clusters.

3.4. HOMO–LUMO Gaps and Charge Transfer

The HOMO–LUMO gap is considered to be an important criterion in terms of the electronic stability of clusters [52]. It represents the ability of a molecule to participate in chemical reactions to some degree. A large HOMO–LUMO energy gap is associated with enhanced chemical stability. For the most stable Si_{n+2} and Au_2Si_n ($n = 1-8$) clusters, the HOMO–LUMO gaps against the cluster size are plotted in Figure 4. As seen from the figure, the tendencies of the HOMO–LUMO gaps for Si_{n+2} clusters are similar to the previ-

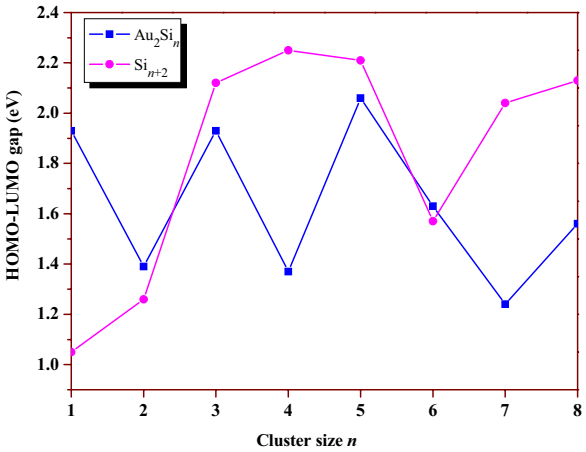

Fig. 4 (colour online). Size dependence of the HOMO–LUMO gaps for the lowest energy structures of Si_{n+2} and Au_2Si_n ($n = 1-8$) clusters.

Table 3. Mulliken charges populations of the lowest energy Au_2Si_n ($n = 1-8$) clusters.

Isomers	Au-1	Au-2	Si-1	Si-2	Si-3	Si-4	Si-5	Si-6	Si-7	Si-8
Au_2Si	−0.316	−0.316	0.632							
Au_2Si_2	−0.443	−0.443	0.443	0.443						
Au_2Si_3	−0.258	−0.519	0.368	0.368	0.041					
Au_2Si_4	−0.747	−0.747	0.621	0.621	0.125	0.125				
Au_2Si_5	−0.835	−0.702	0.403	0.372	0.339	0.303	0.797			
Au_2Si_6	−0.678	−0.595	0.277	−0.281	0.404	0.729	0.461	−0.318		
Au_2Si_7	−1.013	−1.013	−0.671	0.939	0.939	−0.487	0.388	0.200	0.716	
Au_2Si_8	−0.980	−0.948	0.153	0.783	−0.061	0.293	0.340	0.879	0.522	−0.397

Table 4. Natural electronic configurations of the gold atoms in the lowest energy Au_2Si_n ($n = 1-8$) clusters, where Au (1) and Au (2) correspond to the top (or left) and bottom (or right) gold atoms in Figure 1.

Isomer	Au (1)				Au (2)			
	6*s*	5*d*	6*p*	7*p*	6*s*	5*d*	6*p*	7*p*
Au_2Si	1.29	9.77	0.05	0	1.29	9.77	0.05	0
Au_2Si_2	1.05	9.80	0.10	0	1.05	9.80	0.10	0
Au_2Si_3	1.06	9.83	0.01	0	1.03	9.73	0.28	0.01
Au_2Si_4	1.01	9.75	0.24	0.01	1.01	9.75	0.24	0.01
Au_2Si_5	0.96	9.75	0.33	0.01	0.96	9.77	0.24	0.01
Au_2Si_6	1.04	9.75	0.19	0.01	1.05	9.77	0.11	0.01
Au_2Si_7	0.86	9.73	0.56	0.01	0.86	9.73	0.56	0.01
Au_2Si_8	0.89	9.73	0.35	0.01	0.95	9.73	0.43	0.01

ous theoretical results [7, 38, 53]. It is interesting that the HOMO–LUMO gaps for Au_2Si_n clusters exhibit an obvious odd-even oscillation except for the Au_2Si_7 isomer. In particular, Au_2Si_5 has the largest HOMO–LUMO gap of 2.06 eV. This means that the Au_2Si_5 cluster possesses a dramatically enhanced chemical stability and can be seen as the building block of novel nanomaterials.

The net Mulliken populations (MPs) can provide reliable charge-transfer information. Here, the Mulliken populations of the most stable Au_2Si_n ($n = 1-8$) clusters are listed in Table 3. As shown in Table 3, the MPs values for the gold atoms in the Au_2Si_n ($n = 1-8$) clusters are negative, suggesting that the charge in the corresponding cluster transfers from the Si_n framework to gold atoms due to the larger electronega-

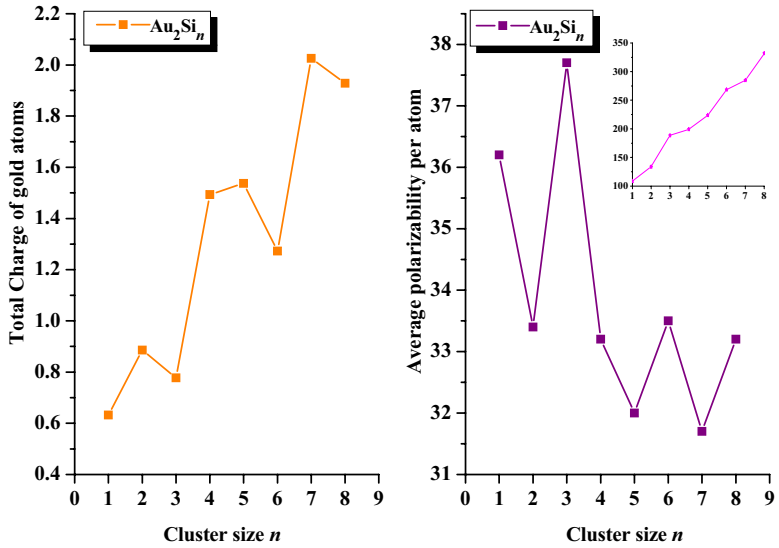

Fig. 5 (colour online). Size dependence of the charge transfer and average polarizability per atom for the lowest energy structures Au_2Si_n ($n = 1-8$) clusters. The polarizability of Au_2Si_n clusters is shown in the inserted figure.

tivity of gold than silicon. This feature is consistent with Mo_2Si_n systems by Han et al. [42]. Moreover, we find that the charges are equal for each gold atom in $Au_2Si_{1,2,4,7}$ clusters, whereas they are different in others. This may be due to the fact that there are an equal number of $Au-Si$ bonds in $Au_2Si_{1,2,4,7}$ clusters. In other words, the charge distribution is dependent on the symmetry of the cluster. In Figure 5, size dependence of the total charges of gold atoms in the Au_2Si_n ($n=1-8$) clusters is given. As shown in the figure, the total charges of gold atoms display a growing trend with the size increasing. There is an obvious odd-even oscillation when $n<5$, while for $n\geq 5$, the inverse odd-even alternation is found. Namely, the gold atoms in clusters with even-numbered clusters attract more charges from the Si_n framework than the even-numbered ones when $n<5$; on the contrary, less charges transfer from the Si_n framework to gold atoms in even-numbered clusters for $n\geq 5$. So the cluster size 5 is a pivotal point. In order to understand the internal charge transfer, the natural electron configurations for the gold atoms in the most stable Au_2Si_n systems are investigated, and these are tabulated in Table 4. It is shown that the $5d$ states lose $0.27-0.17$ electrons, while the $6p$ states get $0.01-0.56$ electrons. For the contribution from the $7p$ states, it is nearly zero.

3.5. Polarizability

It is known that the static polarizability is a measure of the distortion of the electronic density and provides information about the response of the system under the effect of an external static electric field [54]. Here, the average static polarizability is defined as [55]

$$\overline{\alpha}=(\alpha_{xx}+\alpha_{yy}+\alpha_{zz})/3. \tag{6}$$

For the gold and silicon atoms, our calculated values are 34.8 and 23.4 au, respectively. Our results are in reasonable agreement with the reported experimental estimate 39.1 ± 9.8 au [56] for the gold atom and theoretical value 20 au [57] for the silicon atom. In Figure 5, the polarizability and average polarizability per atom ($\overline{\alpha}/n$) of small size Au_2Si_n ($n=1-8$) clusters are exhibited. As shown in the figure, it is clear that the polarizabilities of Au_2Si_n clusters increase as a function of cluster size n, modulated by a slight oscillating behaviour, up to $n=8$. These characteristics of polarizabilities with cluster size are similar to the water clusters reported by Ghanty and Ghosh [58]. It is most interesting to note that the average polarizability per atom displays an absolutely inverse correction comparing with charge transfer. When $n<5$, the $Au_2Si_{2,4}$ clusters possess lower polarizability than $Au_2Si_{1,3}$ isomers, while for $n\geq 5$, the $Au_2Si_{5,7}$ clusters show slighter polar effects than that of $Au_2Si_{6,8}$ clusters. Although the local minimum is not emerged at $n=5$, the Au_2Si_5 clusters are a transition point for our investigated systems. It is consistent with the case of charge transfer.

4. Conclusions

All the results are summarized as follows:

(i) The optimized geometries show that the most stable isomers have 3D structure except for $Au_2Si_{1,3}$ clusters. Among them, the $Au_2Si_{1,4,9}$ clusters can be viewed as a substituted structure of ground state of pure silicon clusters. In addition, we also found that the doped gold atoms prefer to occupy the surface site of Au_2Si_n cluster, which is consistent with the case of single gold doped silicon clusters.

(ii) The averaged atomic binding energies and fragmentation energies exhibit that the Au_2Si_5 isomer is the most stable structure for Au_2Si_n ($n=1-8$) clusters. The HOMO–LUMO gaps show a pronounced even-odd alternation. Especially, the Au_2Si_5 cluster has the largest HOMO–LUMO gap of 2.06 eV.

(iii) Based on the calculated Mulliken populations, it is noticed that the charges in Au_2Si_n ($n=1-8$) clusters transfer from the Si_n frames to doped gold atoms. For the charge transfer, there is an obvious odd-even oscillation when $n<5$, while for $n\geq 5$, the inverse odd-even alternation is found. Besides, the average polarizability per atom of Au_2Si_n has a reverse even–odd alternation rule compared with charge transfer. A transition point appears at $n=5$.

Acknowledgement

The authors would like to thank the Calculating Center of Sichuan University of Science & Engineering providing CPU time.

Appendix A: Higher Energy Structures

The following structures are higher energy isomers for the Au_2Si_n ($n = 1-8$) clusters. The symmetries and relative energies of higher energy isomers are given below them.

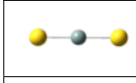		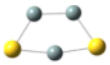		
1c $D_{\infty h}$ 3.74	2e C_{2v} 1.49	3e C_{2v} 0.22	3f C_{2v} 0.49	3g C_{2h} 0.60
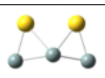	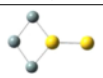			
3h C_S 0.65	3i C_{2v} 0.83	3j C_{2v} 3.57		
				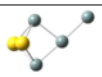
4e C_1 0.66	4f C_{2v} 0.81	4g C_2 1.34	4h C_s 1.41	4i C_s 1.91
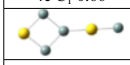	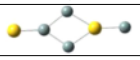			
4j C_{2v} 2.17	4k C_{2v} 2.31			
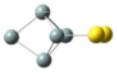			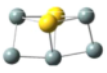	
5e C_s 0.95	5f D_{3h} 1.00	5g C_1 1.34	5h C_2 1.48	5i D_{2h} 1.62
				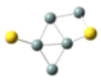
5j D_{5h} 1.66	5k C_S 1.79	5l C_s 2.00	5m C_s 2.00	5n C_1 2.06
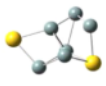	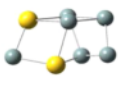	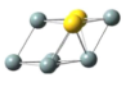	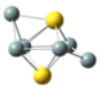	
6e C_1 0.53	6f C_1 0.59	6g C_s 0.93	6h C_s 0.96	6i C_{2v} 1.02
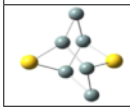		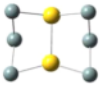	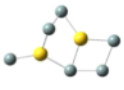	
6j C_1 1.11	6k C_1 1.20	6l C_s 2.29	6m C_1 3.48	6n C_{2v} 3.63
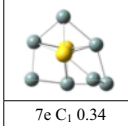	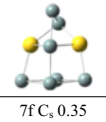	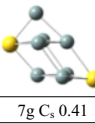	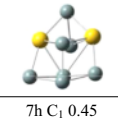	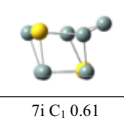
7e C_1 0.34	7f C_s 0.35	7g C_s 0.41	7h C_1 0.45	7i C_1 0.61
7j C_1 0.63	7k C_1 0.65	7l C_1 0.71	7m C_s 1.07	7n C_s 1.18
8e C_1 1.12	8f C_2 1.19	8g C_1 1.39	8h C_s 1.48	8i C_s 1.63
8j C_{2v} 1.68	8k C_1 1.72	8l C_1 1.73	8m C_{2v} 1.91	8n C_S 3.33

Appendix B: Cartesian Coordinates

In following tables, the Cartesian coordinates of the lowest-energy and few low-lying isomers of the Au_2Si_n ($n = 1-8$) clusters for each size are given. The unit of the coordinates is Å.

1. Au_2Si

1a			1b		
0	1.67	0.13	0	0	1.55
0	1.67	0.13	0	0	−3.21
0	0	1.44	0	0	0.98

2. Au_2Si_2

2a			2b			2c			2d			2e		
0	1.60	−0.22	0	0.88	0	0	0	1.58	0	1.13	−2.89	1.00	1.04	1.43
1.19	0	1.25	−1.81	−0.71	0	0	1.80	0	0	−1.13	−2.89	−1.13	1.04	−0.20
−1.19	0	1.25	2.17	0.25	0	0	−1.80	0	0	0	−0.76	1.35	1.04	−1.23
0	−1.60	−0.22	−2.04	1.71	0	0	0	−1.58	0	0	1.78	1.35	−1.64	−1.23

3. Au_2Si_3

3a				3b			3c			3d			3e	
0	1.72	−0.96	0.75	0.25	1.53	−1.30	3.03	0	0.70	−0.39	0	0	2.42	0.26
0	−1.72	−0.96	0.74	0.25	−1.53	1.84	−0.08	0	−0.05	1.80	1.12	0	−2.42	0.26
0	0	2.82	1.14	2.06	0	0	1.26	0	−0.05	1.80	−1.12	0	1.12	−1.75
0	0	−2.58	−1.21	1.15	0	−2.60	1.05	0	−0.05	−0.28	2.30	0	−1.12	−1.75
0	0	0.55	0.75	−1.60	0	−1.15	−0.86	0	−0.05	−0.28	−2.30	0	0	0.55

4. Au_2Si_4

4a				4b			4c			4d			4e	
0.68	1.51	0.22	1.59	1.66	0	−1.62	1.43	−1.29	−1.88	0.51	1.61	−1.24	0	2.59
−0.68	−1.51	0.22	1.33	−0.69	0	0.77	1.40	−0.96	−1.61	2.63	−0.59	1.24	0	2.59
1.59	−0.68	−0.40	−0.22	1.92	1.41	−0.77	1.40	0.96	−2.60	0.55	−0.73	0	1.67	1.57
−1.59	0.68	−0.40	−0.22	1.92	−1.41	2.09	−0.50	−0.11	0.01	1.42	0.42	0	−1.67	1.57
0.68	−0.95	2.06	−0.22	−0.43	1.83	1.62	1.43	1.29	1.89	0.16	−0.03	0	−1.35	−0.74
−0.68	0.95	2.06	0	−0.43	−1.83	−2.09	−0.50	0.11	−0.81	−1.07	−0.10	0	1.35	−0.74

5. Au_2Si_5

5a				5b			5c			5d			5e	
−1.64	1.88	−0.63	−1.04	0.59	−1.32	0	1.44	−0.34	0.62	−0.86	1.66	1.93	−1.38	1.42
0.51	1.19	−1.34	0	0	1.32	0	−1.44	−0.34	0.62	−0.86	−1.66	1.93	−1.38	−1.42
0.22	2.38	0.87	0	−2.18	0.30	1.58	0	−1.43	1.79	0.39	0	3.48	−2.48	0
1.43	−0.79	−0.09	2.17	1.05	0.08	−1.58	0	−1.43	−0.79	0.11	0	1.93	0.47	0
2.37	1.61	0.06	−2.17	−1.05	0.08	0	0	1.42	−1.22	2.43	0	0.18	−1.98	0
−0.02	0.11	1.61	0	2.18	0.30	0	0	3.68	1.17	2.59	0	−1.62	−0.49	0
−1.69	−0.48	−0.01	1.04	−0.59	−1.32	0	0	−3.30	0.62	−2.67	0	−0.06	1.69	0

6. Au_2Si_6

6a				6b			6c			6d			6e	
−0.85	−1.23	1.11	−0.12	−0.09	2.03	0	1.63	1.58	0.58	1.05	1.92	0.79	2.17	0.84
−0.02	1.08	1.38	−1.30	−0.09	0	0	1.26	−1.34	0.58	1.05	−1.92	−1.21	1.00	1.40
2.11	1.75	0.53	1.18	−0.09	0	0	−1.63	1.58	−0.58	−1.05	−1.92	−1.19	2.79	−0.36
0.40	−0.29	−0.70	−0.12	−0.09	−2.03	0	−1.26	−1.34	−0.58	−1.05	1.92	−1.15	−1.11	0
−2.74	−0.41	−0.14	−0.12	−0.09	−1.87	−1.32	0	0.37	0.58	−2.25	0	−2.85	1.07	−0.33
−1.92	1.84	0.10	−0.12	−0.09	1.87	1.32	0	0.37	−1.48	0.01	0	−0.29	0.82	−1.32
2.75	−0.51	−0.10	1.61	−0.09	0	0	3.35	−0.11	−0.58	2.25	0	1.82	0.09	−0.10
0.23	1.99	−1.04	−1.50	−0.09	0	0	−3.35	−0.11	1.48	−0.01	0	0.99	−2.05	0.34

7. Au_2Si_7

7a				7b			7c			7d			7e	
1.99	2.20	0	−0.68	−1.23	1.28	−0.92	−1.43	−0.50	0	2.00	2.57	−0.84	−1.12	2.28
−0.09	1.91	1.29	−0.25	1.16	1.46	1.20	−1.98	0.62	0	1.39	0.10	−0.05	1.02	1.48
−0.09	1.91	−1.29	1.77	1.84	0.31	0.23	−0.07	1.62	0	−1.39	0.10	0.51	−2.07	0.52
−1.84	2.69	0	−0.23	0.15	−0.92	1.76	1.65	0.93	0	−2.00	2.57	0.38	−1.49	−1.84
−1.92	0.20	0	−2.60	−0.49	−0.13	−1.40	1.30	0.61	0	0	3.97	0.18	1.15	−1.50
1.92	−0.17	0	−2.16	1.92	0.34	0.41	0.41	−0.97	1.31	0	1.91	−1.39	−0.47	−0.25
−0.09	−0.57	−1.54	2.75	−0.29	−0.03	0.09	2.73	−0.63	−1.31	0	1.91	1.74	0.06	0.06
−0.09	−0.57	1.54	−0.24	2.43	−1.06	−3.07	−0.21	−0.09	1.62	0	−1.16	−2.09	1.79	−0.06
1.01	−2.33	0	−1.84	−1.84	−0.51	2.82	−0.25	−0.21	−1.62	0	−1.16	−0.04	3.03	0.16

8. Au_2Si_8

8a				8b			8c			8d			8e	
−0.77	1.71	−1.68	0.80	−0.65	1.68	−0.75	0.07	1.61	−1.12	−0.39	0.88	0.51	0.64	1.42
1.51	0.98	−1.41	0.96	−1.72	−1.33	0.59	−0.10	−1.05	1.12	0.39	0.88	1.48	2.32	−0.20
0.35	2.60	0.16	−2.19	1.98	0.20	0.23	2.13	0.49	0.60	−2.05	1.66	−2.72	1.38	−0.47
1.23	−1.21	−0.41	1.77	2.13	−0.03	−2.00	1.67	−0.57	0.74	−1.03	−1.23	−1.05	2.34	0.99
2.70	2.23	0.25	−0.08	1.74	1.35	−0.30	−2.16	−0.23	0.60	2.84	−0.30	−0.45	1.09	−1.08
1.39	0.54	1.41	−0.33	2.52	−1.20	−1.74	2.27	1.75	−0.60	−2.84	−0.30	2.89	0.95	1.19
−1.81	−0.12	−0.38	−0.67	−2.04	0.37	1.19	−1.23	1.47	−0.60	2.05	1.66	−0.05	−1.11	−0.08
−0.58	−1.61	1.13	−0.25	0.26	−0.78	0.05	2.10	−1.86	−0.74	1.03	−1.23	−2.51	−1.03	0.09
−1.25	1.28	0.59	2.51	−0.29	−0.02	2.76	−0.11	−0.06	−2.61	1.27	0.38	2.44	−0.98	−0.26
−0.07	−0.26	3.00	−2.51	−0.46	−0.03	−2.28	−0.73	−0.22	2.61	−1.27	0.38	−0.22	3.74	−0.83

[1] I. Rata, A. A. Shvartsburg, M. Horoi, T. Frauenheim, K. W. M. Siu, and K. A. Jackson, Phys. Rev. Lett. **85**, 546 (2000).
[2] C. C. Arnold and D. M. Neumark, J. Chem. Phys. **99**, 3353 (1993).
[3] K. M. Ho, A. A. Shvartsburg, B. Pan, Z. Y. Lu, C. Z. Wang, J. G. Wacker, J. L. Fye, and M. F. Jarrold, Nature **392**, 582 (1998).
[4] R. Schäfer, S. Schlecht, J. Woenckhaus, and J. A. Becker, Phys. Rev. Lett. **76**, 471 (1996).
[5] S. Vijayalakshmi, M. A. George, and H. Grebel, Appl. Phys. Lett. **70**, 708 (1997).
[6] B. Liu, Z. Y. Lu, B. Pan, C. Z. Wang, and K. M. Ho, J. Chem. Phys. **109**, 9401 (1998).
[7] C. Pouchan, D. Bégué, and D. Y. Zhang, J. Chem. Phys. **121**, 4628 (2004).
[8] D. Bégué, G. Maroulis, and C. Pouchan, J. Chem. Phys. **119**, 794 (2003).
[9] A. Tekin and B. Hartke, Phys. Chem. Chem. Phys. **6**, 503 (2004).
[10] A. D. Zdetsis, J. Chem. Phys. **127**, 244308 (2007).
[11] J. C. Yang, W. G. Xu, and W. S. Xiao, J. Mol. Struct. (Theochem) **719**, 89 (2005).
[12] K. Raghavachari and C. M. Rohlfing, J. Chem. Phys. **89**, 2219 (1988).
[13] E. Janssens, P. Gruene, G. Meijer, L. Wöste, P. Lievens, and A. Fielicke, Phys. Rev. Lett. **99**, 063401 (2007).
[14] S. M. Beck, J. Chem. Phys. **90**, 6306 (1989).
[15] H. Hiura, T. Miyazaki, and T. Kanayama, Phys. Rev. Lett. **86**, 1733 (2001).
[16] J. J. Scherer, J. B. Paul, C. P. Collier, and R. J. Saykally, J. Chem. Phys. **102**, 5190 (1995).
[17] J. J. Scherer, J. B. Paul, C. P. Collier, and R. J. Saykally, J. Chem. Phys. **103**, 9187 (1995).
[18] J. J. Scherer, J. B. Paul, C. P. Collier, and R. J. Saykally, J. Chem. Phys. **103**, 113 (1995).
[19] H. G. Xu, Z. G. Zhang, Y. Feng, J. Y. Yuan, Y. C. Zhao, and W. J. Zheng, Chem. Phys. Lett. **487**, 204 (2010).
[20] H. G. Xu, Z. G. Zhang, Y. Feng, and W. J. Zheng, Chem. Phys. Lett. **498**, 22 (2010).
[21] J. Lu and S. Nagase, Phys. Rev. Lett. **90**, 115506 (2003).
[22] P. Turski, Chem. Phys. Lett. **315**, 115 (1999).
[23] P. Turski and M. Barysz, J. Chem. Phy. **113**, 4654 (2000).
[24] V. Kumar and Y. Kawazoe, Phys. Rev. Lett. **87**, 045503 (2001).
[25] H. Kawamura, V. Kumar, and Y. Kawazoe, Phys. Rev. B **71**, 075423 (2005).
[26] V. Kumar and Y. Kawazoe, Phys. Rev. Lett. **90**, 055502 (2003).
[27] A. K. Singh, T. M. Briere, V. Kumar, and Y. Kawazoe, Phys. Rev. Lett. **91**, 146802 (2003).
[28] A. D. Zdetsis, Phys. Rev. B **75**, 085409 (2007).
[29] A. D. Zdetsis, Phys. Rev. A **64**, 023202 (2001).
[30] J. G. Han and F. Hagelberg, Chem. Phys. **263**, 255 (2001).
[31] J. G. Han, C. Xiao, and F. Hagelberg, Struct. Chem. **13**, 173 (2002).

[32] J. G. Han and F. Hagelberg, Chem. Phys. **286**, 181 (2003).
[33] P. F. Zhang, J. G. Han, and Q. R. Pu, J. Mol. Struct. (Theochem) **635**, 25 (2003).
[34] P. Guo, Z. Y. Ren, F. Wang, J. Bain, J. G. Han, and G. H. Wang, J. Chem. Phys. **121**, 12265 (2004).
[35] J. G. Han, Z. Y. Ren, and B. Z. Lu, J. Phys. Chem. A **108**, 5100 (2004).
[36] J. Wang and J. G. Han, J. Chem. Phys. **123**, 064306 (2005).
[37] B. Kiran, X. Li, H. J. Zhai, L. F. Cui, and L. S. Wang, Angew. Chem. Int. Ed. **43**, 2125 (2004).
[38] J. Wang, Y. Liu, and Y. C. Li, Phys. Lett. A **374**, 2736 (2010).
[39] R. Robles and S. N. Khanna, J. Chem. Phys. **130**, 164313 (2009).
[40] R. Robles and S. N. Khanna, Phys. Rev. B **77**, 235441 (2008).
[41] X. Li, B. Kiran, and L. S. Wang, J. Phys. Chem. A **109**, 4366 (2005).
[42] J. G. Han, R. N. Zhao, and Y. H. Duan, J. Phys. Chem. A **111**, 2148 (2007).
[43] M. J. Frisch, G. W. Trucks, H. B. Schlegel, G. E. Scuseria, M. A. Robb, J. R. Cheeseman, J. A. Montgomery, Jr., T. Vreven, K. N. Kudin, J. C. Burant, J. M. Millam, S. S. Iyengar, J. Tomasi, V. Barone, B. Mennucci, M. Cossi, G. Scalmani, N. Rega, G. A. Petersson, H. Nakatsuji, M. Hada, M. Ehara, K. Toyota, R. Fukuda, J. Hasegawa, M. Ishida, T. Nakajima, Y. Honda, O. Kitao, H. Nakai, M. Klene, X. Li, J. E. Knox, H. P. Hratchian, J. B. Cross, V. Bakken, C. Adamo, J. Jaramillo, R. Gomperts, R. E. Stratmann, O. Yazyev, A. J. Austin, R. Cammi, C. Pomelli, J. Ochterski, P. Y. Ayala, K. Morokuma, G. A. Voth, P. Salvador, J. J. Dannenberg, V. G. Zakrzewski, S. Dapprich, A. D. Daniels, M. C. Strain, O. Farkas, D. K. Malick, A. D. Rabuck, K. Raghavachari, J. B. Foresman, J. V. Ortiz, Q. Cui, A. G. Baboul, S. Clifford, J. Cioslowski, B. B. Stefanov, G. Liu, A. Liashenko, P. Piskorz, I. Komaromi, R. L. Martin, D. J. Fox, T. Keith, M. A. Al-Laham, C. Y. Peng, A. Nanayakkara, M. Challacombe, P. M. W. Gill, B. G. Johnson, W. Chen, M. W. Wong, C. Gonzalez, and J. A. Pople, GAUSSIAN 03 (Revision E.01), Gaussian, Inc., Wallingford, CT, 2004.
[44] J. Tao, J. P. Perdew, V. N. Staroverov, and G. E. Scueria, Phys. Rev. Lett. **91**, 146401 (2003).
[45] R. Krishnan, J. S. Binkley, R. Seeger, and J. A. Pople, J. Chem. Phys. **72**, 650 (1980).
[46] P. J. Hay and W. R. Wadt, J. Chem. Phys. **82**, 299 (1985).
[47] K. P. Huber and G. Herzberg, Constants of Diatomic Molecules, Van Nostrand Reinhold Press, New York 1979.
[48] D. R. Stull and H. Prophet, JANAF Thermochemical Table, NSRDS Natl. Stand. Ref. Data Serv. Natl. Bur. Stand, No. 37, U. S. GPO, Washington, D.C. 1971.
[49] K. Raghavachari, J. Chem. Phys. **84**, 5672 (1986).
[50] E. C. Pattersan and R. P. Messmer, Phys. Rev. B **42**, 7530 (1990).
[51] A. A. Hoops, R. T. Bise, H. Choi, and D. M. Neumark, Chem. Phys. Lett. **346**, 89 (2001).
[52] A. B. Sannigrahi, P. K. Nandi, and P. v. R. Schleyer, J. Am. Chem. Soc. **116**, 7225 (1994).
[53] L. Ma, J. J. Zhao, J. G. Wang, Q. L. Lu, L. Z. Zhu, and G. H. Wang, Chem. Phys. Lett. **411**, 279 (2005).
[54] K. R. S. Chandrakumar, T. K. Ghanty, and S. K. Ghosh, J. Phys. Chem. A **108**, 6661 (2004).
[55] K. Gupta, T. K. Ghanty, and S. K. Ghosh, Phys. Chem. Chem. Phys. **12**, 2929 (2010).
[56] B. O. Roos, R. Liudh, P. A. Malmqvist, V. Veryazov, and P. O. Widmark, J. Phys. Chem. A **109**, 6575 (2005).
[57] M. Guillaume, B. Champagne, D. Bégué, and C. Pouchan, J. Chem. Phys. **130**, 134715 (2009).
[58] T. K. Ghanty and S. K. Ghosh, J. Chem. Phys. **118**, 8547 (2003).